INTERNATIONAL JOURNAL OF OPTIMIZATION IN CIVIL ENGINEERING
Int. J. Optim. Civil Eng., 2025; 15(2):203-219

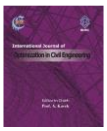

OPTIMAL DESIGN OF DOUBLE-TMDI FOR SEISMIC CONTROL OF BUILDINGS UNDER SOIL-STRUCTURE INTERACTION BY OPPOSITION-SWITCHING SEARCH

M. Shahrouzi[*, †1], M. Fahimi Farzam[2], and J. Gholizadeh[1]
1. Civil Engineering Department, Faculty of Engineering, Kharazmi University, Tehran, Iran
2. Civil Engineering Department, Faculty of Engineering, University of Maragheh, Maragheh, Iran

ABSTRACT

The tuned mass damper inerter systems have recently received considerable attention in the field of structural control. The present work offers a practical configuration of such a device, called double tuned mass damper inerter (DTMDI) that connects the inerter into the damper masses rather than be attached to the main structure. Soil-structure interaction is also taken into account for the soft and dense soils as well as for the fixed based condition. The H_∞ norm of the transfer functions for the roof response is minimized as the objective function. The parameters of DTMDI are optimized using opposition-switching search as an efficient parameter-less algorithm in comparison with lightning attachment procedure optimization, sine cosine algorithm and particle swarm optimization. The system performance is evaluated in the frequency domain, as well as in the time domain under various earthquakes including far-field records, near-field records with forward directivity and with fling-step. The results show superiority of opposition-switching search for optimal design of the proposed DTMDI so that it can significantly reduce both the roof displacement and acceleration response for all the SSI conditions.

Keywords: Double tuned mass damper inerter, Soil-structure interaction, Opposition-switching-search, Meta-heuristic algorithms, Robust seismic control.

Received: 18 March 2025; Accepted: 22 May 2025

[*]Corresponding author: Faculty of Engineering, Kharazmi University, Tehran & Karaj, Iran
[†]E-mail address: shahruzi@khu.ac.ir (M. Shahrouzi)

1. INTRODUCTION

Structures may experience significant vibrations under dynamic loadings such as wind and earthquake. Such vibrations can be mitigated using structural control systems, which are generally classified into four categories: active, passive, semi-active, and hybrid control. Although the active and semi-active control systems initially appeared promising, challenges such as the need for advanced technology, high maintenance costs, and reliability concerns have led the researchers to focus more on passive control systems due to their simplicity. Passive devices are added to the main structure to protect it by reducing the input energy [1].

For years, increasing the TMD mass has been a popular passive control solution, while a few buildings incorporated large TMD's on dedicated floors. Such large masses can pose architectural and structural stability issues, for which the inerter is a solution.

Since the frequency ratio of TMD's is defined based on the structure's natural frequency, and the underlying soil significantly affects the fundamental mode, *Soil–Structure Interaction* (SSI) plays a crucial role in tuning such a control system. Bekdaş et al. [2] investigated a 40-story building equipped with a TMD, considering SSI. Kaveh et al. [3] applied a Chaotic Optimization Algorithm for tuning TMD in 10-story and 76-story buildings.

Metaheuristic algorithms have been widely used for engineering problems [4–8]. Kamgar et al. utilized whale optimization algorithm for design of TMD considering soil-structure interaction [9]. Kaveh et al. applied charged system search for optimal design of TMD in benchmark examples [10]. Bekdas et al. tested three metaheuristic algorithms for optimization of TMD considering frequecy domain [11]. Khatibinia et al. applied multi-objective particle swarm optimizer to tune TMD in the 40-story building [12].

Recently, tuned mass damper inerter (TMDI) has been introduced, attracting widespread attention in the field of structural control [13]. A TMDI consists of a classical TMD combined with a mechanical two-terminal device called an inerter. The inerter, introduced by Smith in 2002, can generate a force proportional to the relative acceleration between its terminals [14]. In essence, it can create a virtual mass without adding actual physical weight. Some investigators have thus suggested connecting the second terminal of the inerter to building floors [15], adjacent structures [16], or seismic isolators [17].

To overcome the connection challenges, it was offered to combine the inerter with a double tuned mass damper (DTMDI) [18,19]. The configuration has shown promising results without requiring direct attachment to specific building floors. Nevertheless, most TMDI-related studies have neglected the effects of soil flexibility. Elias and Djerouni analyzed a TMDI-equipped structure subjected to far-field and near-field ground motions, considering SSI [20]. Their findings demonstrated that the TMDI remains effective in reducing structural responses even when SSI is accounted for.

The present study investigates performance of optimally designed DTMDI system under soil–structure interaction. As a case study, a 15-story shear building is analyzed considering three conditions; i.e. the Fixed base, the dense soil, and the soft soil beneath the foundation. The DTMDI parameters are optimized using four metaheuristic algorithms including *Opposition-Switching Search* (OSS) [21–23], *Lightning Attachment Procedure Optimization* (LAPO) [24], *Sine Cosine Algorithm* (SCA) [25] and *Particle Swarm Optimization* (PSO) [26]. The optimization objective is to minimize the norm H_∞ of the transfer function

for the top displacement. The optimally designed DTMDI is further evaluated in frequency- and time-domain under a variety of earthquake excitations; categorized into far-field records, near-field with forward directivity, and near-field with fling-step.

2. EQUATIONS OF MOTION WITH SOIL–STRUCTURE INTERACTION

The equation of motion for an N-degree-of-freedom shear building without control, subjected to seismic excitation, can be expressed as follows:

$$[\mathbf{M_t}]\ddot{\mathbf{u}}_\mathbf{t}(t)+[\mathbf{C_t}]\dot{\mathbf{u}}_t(t)+[\mathbf{K}_t]\mathbf{u_t}(t)=-\mathbf{F}(t) \tag{1}$$

where M_t, C_t, and K_t represent the mass, damping, and stiffness matrices of the structure, respectively. $F(t)$ represents the external force vector due to ground motion. The vectors $\ddot{u}_t$, $\dot{u}_t$, and u_t denote the floor acceleration, velocity, and displacement, respectively. The dimensions of the matrices and vectors may vary depending on whether SSI or control systems are considered.

To incorporate SSI into the dynamics of the uncontrolled structure, the properties of the soil are added to the mass, damping, and stiffness matrices. The updated matrices and external force and response vectors are defined as per Equations (2) through (6).

$$\mathbf{M_t}=\begin{bmatrix}\mathbf{M}_{n\times n} & \mathbf{M}\mathbf{r}_{n\times 1} & \mathbf{M}\mathbf{z}_{n\times 1}\\ \mathbf{r}^T\mathbf{M}_{1\times n} & \mathbf{r}^T\mathbf{M}\mathbf{r}+m_f & \sum m_i z_i\\ \mathbf{z}^T\mathbf{M}_{1\times n} & \sum m_i z_i & I_f+\sum(m_i z_i+I_i)\end{bmatrix}_{(n+2\times n+2)} \tag{2}$$

$$\mathbf{C_t}=\begin{bmatrix}\mathbf{C}_{n\times n} & \mathbf{0}_{n\times 1} & \mathbf{0}_{n\times 1}\\ \mathbf{0}_{1\times n} & c_h & 0\\ \mathbf{0}_{1\times n} & 0 & c_\theta\end{bmatrix}_{(n+2\times n+2)} \tag{3}$$

$$\mathbf{K_t}=\begin{bmatrix}\mathbf{K}_{n\times n} & \mathbf{0}_{n\times 1} & \mathbf{0}_{n\times 1}\\ \mathbf{0}_{1\times n} & k_h & 0\\ \mathbf{0}_{1\times n} & 0 & k_\theta\end{bmatrix}_{(n+2\times n+2)} \tag{4}$$

$$\mathbf{F}=\begin{Bmatrix}\mathbf{M}\mathbf{r}_{n\times 1}\\ \mathbf{r}^T\mathbf{M}\mathbf{r}+m_f\\ \mathbf{z}^T\mathbf{M}\mathbf{r}\end{Bmatrix}_{(n+2)\times 1} \tag{5}$$

$$\ddot{\mathbf{u}}_{\mathbf{t}} = \begin{Bmatrix} \ddot{\mathbf{u}}_{n\times1} \\ \ddot{u}_f \\ \theta \end{Bmatrix}_{(n+2)\times1}, \dot{\mathbf{u}}_{\mathbf{t}} = \begin{Bmatrix} \dot{\mathbf{u}}_{n\times1} \\ \dot{u}_f \\ \theta \end{Bmatrix}_{(n+2)\times1}, \mathbf{u}_{\mathbf{t}} = \begin{Bmatrix} \mathbf{u}_{n\times1} \\ u_f \\ \theta \end{Bmatrix}_{(n+2)\times1} \tag{6}$$

$\boldsymbol{M}$, $\boldsymbol{C}$, and $\boldsymbol{K}$ denote the mass, damping, and stiffness matrices of the uncontrolled structure. The vector $\boldsymbol{r}$ is a unit vector of appropriate dimension. Z_i denotes the absolute height of each floor relative to the foundation. m_f, I_f, u_f, and θ represent the mass, moment of inertia, displacement, and rotation of the foundation, respectively. m_i and I_i are the mass and moment of inertia of each floor. The horizontal and rotational damping are represented by c_h and c_θ, respectively, and the corresponding stiffness terms by k_h and k_θ.

In the present study, the structure is controlled using a Double Tuned Mass Damper Inerter (DTMDI). Fig. 1 illustrates the uncontrolled and DTMDI-controlled structures under the influence of soil–structure interaction.

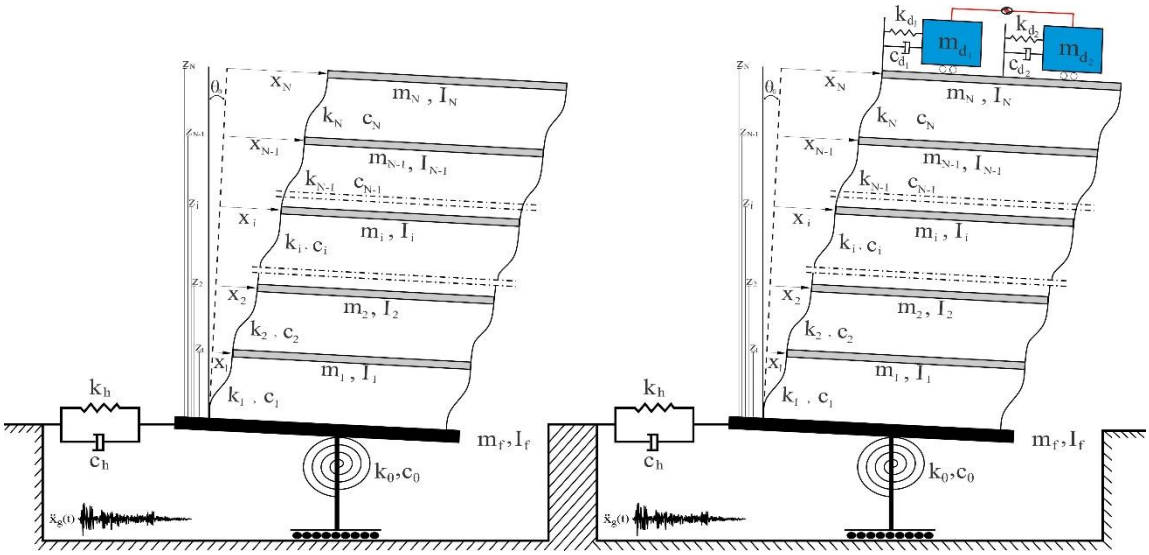

Figure 1: Uncontrolled (left) and DTMDI-controlled (right) building model considering soil–structure interaction

The governing equations for the DTMDI-controlled structure are redefined accordingly, where the contribution of the inerter element is incorporated into the mass matrix.

$$\mathbf{M}_{\mathbf{t}} = \begin{bmatrix} \mathbf{M}_{(n+2)\times(n+2)} & \mathbf{M}\mathbf{r}_{(n+2)\times1} & \mathbf{M}\mathbf{z}_{(n+2)\times1} \\ \mathbf{r}^T\mathbf{M}_{(1\times n+2)} & \mathbf{r}^T\mathbf{M}_{(n+2)\times(n+2)}\mathbf{r} + m_f & \sum m_i z_i \\ \mathbf{z}^T\mathbf{M}_{1\times(n+2)} & \sum m_i z_i & I_f + \sum_{i=1}^{n}(m_i z_i + I_i) \end{bmatrix}_{(n+4)\times(n+4)} \tag{7}$$

$$\mathbf{C}_{\mathbf{t}} = \begin{bmatrix} \mathbf{C}_{(n+2)\times(n+2)} & \mathbf{0}_{(n+2)\times 1} & \mathbf{0}_{(n+2)\times 1} \\ \mathbf{0}_{1\times(n+2)} & c_h & 0 \\ \mathbf{0}_{1\times(n+2)} & 0 & c_\theta \end{bmatrix}_{(n+4)\times(n+4)} \tag{8}$$

$$\mathbf{K}_{\mathbf{t}} = \begin{bmatrix} \mathbf{K}_{(n+2)\times(n+2)} & \mathbf{0}_{(n+2)\times 1} & \mathbf{0}_{(n+2)\times 1} \\ \mathbf{0}_{1\times(n+2)} & k_h & 0 \\ \mathbf{0}_{1\times(n+2)} & 0 & k_\theta \end{bmatrix}_{(n+4)\times(n+4)} \tag{9}$$

$$\mathbf{F} = \begin{Bmatrix} \mathbf{M}\mathbf{r}_{(n+2)\times 1} \\ \mathbf{r}^T\mathbf{M}_{(n+2)\times(n+2)}\mathbf{r}_{(n+2)\times 1} + m_f \\ \mathbf{z}^T\mathbf{M}_{(n+2)\times(n+2)}\mathbf{r} \end{Bmatrix}_{(n+4)\times 1} \tag{10}$$

$$\ddot{\mathbf{u}}_{\mathbf{t}} = \begin{Bmatrix} \ddot{\mathbf{u}}_{(n+2)\times 1} \\ \ddot{u}_f \\ \theta \end{Bmatrix}_{(n+4)\times 1}, \dot{\mathbf{u}}_{\mathbf{t}} = \begin{Bmatrix} \dot{\mathbf{u}}_{(n+2)\times 1} \\ \dot{u}_f \\ \theta \end{Bmatrix}_{(n+4)\times 1}, \mathbf{u}_{\mathbf{t}} = \begin{Bmatrix} \mathbf{u}_{(n+2)\times 1} \\ u_f \\ \theta \end{Bmatrix}_{(n+4)\times 1} \tag{11}$$

These equations can be rewritten in the state-space form as:

$$\dot{\mathbf{Z}}(t) = \mathbf{A}\mathbf{Z}(t) + \mathbf{B}\ddot{\mathbf{X}}_g(t) \tag{12}$$

Here, $\boldsymbol{Z(t)}$ is the state vector, $\ddot{\boldsymbol{x}}_{\boldsymbol{g}}(t)$ is the ground acceleration input, and matrices $\boldsymbol{A}$ and $\boldsymbol{B}$ are the system and location matrices, respectively. They are defined as:

$$\mathbf{Z}(t) = \begin{bmatrix} \mathbf{x}(t) \\ \dot{\mathbf{x}}(t) \end{bmatrix} \tag{13}$$

$$\mathbf{A} = \begin{bmatrix} \mathbf{0} & \mathbf{I} \\ -\mathbf{M}^{-1}\mathbf{K} & -\mathbf{M}^{-1}\mathbf{C} \end{bmatrix}, \mathbf{B} = \begin{bmatrix} \mathbf{0} \\ -\mathbf{M}^{-1}\mathbf{m}_{\mathbf{g}}\mathbf{r}_{\mathbf{g}} \end{bmatrix} \tag{14}$$

Where $\mathbf{0}$ and $\boldsymbol{I}$ are zero and identity matrices, respectively. The generalized mass matrix $\boldsymbol{m_g}$ and input vector $\boldsymbol{r_g}$ are defined based on the degrees of freedom of the system including both SSI and DTMDI effects.

$$\mathbf{m}_{\mathbf{g}} = \begin{bmatrix} \mathbf{M}_{(N+2)\times(N+2)} & \mathbf{0}_{(N+2)\times 1} & \mathbf{0}_{(N+2)\times 1} \\ \mathbf{0}_{1\times(N+2)} & m_f + \mathbf{r}^T\mathbf{M}\mathbf{r} & 0 \\ \mathbf{0}_{1\times(N+2)} & 0 & \sum(\mathbf{M}\mathbf{Z}) \end{bmatrix} \tag{15}$$

$$\mathbf{r_g} = \begin{bmatrix} 1 & 1 & \dots & 1 \end{bmatrix}_{1\times(N+4)} \tag{16}$$

3. PROBLEM FORMULATION AND THE SOLUTION ALGORITHM

Proper selection of the mass, stiffness, and damping parameters of DTMDI is crucial to fully exploit its potential. Therefore, three key parameters—mass ratio, damping ratio, and frequency ratio—are defined for each mass element of the DTMDI system. Due to practical limitations and the mechanical nature of the inerter device, the mass ratio can be assumed to be small, and only the optimal damping and frequency ratios are sought. In this study, the total mass ratio of the DTMDI system is set to 1% of the total structural mass. It is equally distributed between the two masses. The selected parameters are summarized in Table 1.

Table 1: Optimization variable definitions and variable ranges.

Preselected variables	Optimization variables	The limiting range of the variables
$\frac{m_d}{M} = \mu_1 + \mu_2 = 0.01$	$f_{d1} = \frac{\omega_{d1}}{\omega_{1s}} = \frac{\sqrt{\frac{k_{d1}}{m_{d1}+b}}}{\sqrt{\frac{K}{M}}}, \zeta_{d1} = \frac{c_{d1}}{2(m_{d1}+b)\omega_{d1}}$	$f_{d1} = f_{d2} = [0.01, 2]$
$\beta = \frac{b}{M} = 0.1$	$f_{d2} = \frac{\omega_{d2}}{\omega_{1s}} = \frac{\sqrt{\frac{k_{d2}}{m_{d2}+b}}}{\sqrt{\frac{K}{M}}}, \zeta_{d2} = \frac{c_{d2}}{2(m_{d2}+b)\omega_{d2}}$	$\zeta_{d1} = \zeta_{d2} = [0, 2]$

In recent years, the advancement of computational techniques has brought metaheuristic algorithms into focus for TMD parameter optimization. These algorithms are generally classified into single-agent and population-based methods, with the latter showing greater success. Hence, four population-based metaheuristic algorithms are utilized in this study to optimize the DTMDI system parameters. The optimization objective is to minimize the norm H_∞ of the transfer functions for roof displacement.

The transfer function of the governing equation for an N-degree-of-freedom DTMDI-controlled building under SSI is defined as:

$$G(s) = \mathbf{C}_\mathbf{y}(j\omega\mathbf{I} - \mathbf{A})^{-1}\mathbf{B} \tag{17}$$

where $j = \sqrt{-1}$, ω is the complex frequency variable and $\boldsymbol{C_y}$ is the output matrix used to extract roof displacement, defined as:

$$\mathbf{C}_\mathbf{y} = [[0 \quad \dots \quad 0_{n-1} \quad 1 \quad 0 \quad 0 \quad 0 \quad 0]_{1\times(n+4)} \quad 0_{1\times(n+4)}]_{1\times 2(n+4)} \tag{18}$$

Here, four additional degrees of freedom are considered: two for SSI and two for

DTMDI. The objective is defined as the minimization of norm H_∞ of the transfer function. Hence, the optimization problem is formulated as:

$$\begin{aligned} &\min_{X} \quad \left\| G(j\omega; X) \right\|_\infty \\ &s.t. \\ &\quad X_{\min} \le X \le X_{\max} \end{aligned} \tag{19}$$

For solution of the problem, OSS (a powerful metaheuristic) is utilized in comparison with some other algorithms. They include *Lightning Attachment Procedure Optimization* (LAPO) [24], *Sine Cosine Algorithm* (SCA) [25,27] and *Particle Swarm Optimization* (PSO) [26]. The fair comparison conditions are addressed [27–29] ensuring that the initial population is identically shared between the algorithms in every independent run.

The population size of 30 and prescribed number of 4000 function evaluations are applied for the current research work. PSO is implemented with extra parameters of 1, 2 and 2 for the inertial, cognitive and social factors, respectively.

3.1 Opposition-Switching Search (OSS)

Opposition-Based Learning (OBL) is an emerging technique in the field of artificial intelligence and soft computing [30]. It leverages both an individual and its opposition to enhance exploration of an optimizer in the search space without extra computational effort. Based on the OBL concepts, Shahrouzi [21] has developed a meta-heuristic algorithm; called Opposition-Switching Search (OSS) that employs the following features:

- Information sharing between the search-agents through a pseudo-mean solution. It utilizes a special type of crossover; that is picking up any of its components from randomly chosen members of the population.
- Switching between such a solution and its opposite position as the starting point for walking through the search space
- Elitist strategy by taking the best-so-far solution, X_{Gb} , as the target for further walks

The proposed OSS is, thus, presented via simple algorithmic steps as:

- Generate a randomly positioned population of n individuals, and evaluate their cost function.
- Repeat the following steps for each individual:
  - Calculate an individual Y by the proposed crossover on the entire population
  - Switch the pseudo-mean Z to either Y or its opposite $\tilde{Y}$, by equal chance. Several types of opposition have already been developed in literature [31]. Here, a simple definition is applied for opposite of a design vector Y as:

$$\tilde{Y} = X^L + X^U - Y \tag{20}$$

    in which X^L and X^U are the lower and upper bounds on the design vector, respectively.
  - Take the first walk direction as V_1:

$$V_1 = rand \otimes (X_{Gb} - Z) \tag{21}$$

- Generate the vectors S_1 or S_2 by:

$$S_1 = rand \otimes (X_{Gb} - X_i) \tag{22}$$

$$S_2 = rand \otimes (\tilde{X}_i - X_{Gb}) \tag{23}$$

- Provide the second walk direction V_2 by randomly switching between S_1 and S_2
- Generate the candidate solution $X_{c,i}$ by Equation 24 and evaluate its cost:

$$X_{c,i} = X_i + V_1 + V_2 \tag{24}$$

- Replace the current individual X_i by the candidate solution $X_{c,i}$ if it has lower cost than the current.

- Exit the loop and identify the updated X_{Gb} as the optimum as soon as termination criterion is met; For example, reaching the function calls to the prescribed number of function evaluations: NFE_{max}.

A MATLAB code of OSS is given in the Appendix so that interested users can adopt it for their specific problems. It is given in special format to easily apply fair comparison conditions.

4. OPTIMAL DESIGN OF THE CONTROL SYSTEM

The control system is optimized using the norm H_∞ of the transfer functions for roof displacement as the cost (objective) function. The adopted optimization framework follows a robust control strategy, making it independent of any specific excitation.

Table 2 represents the optimization results obtained from each algorithm. It reveals that the proposed OSS has achieved the least cost (objective value), along with favorable mean and standard deviation of the responses, rendering its results more consistent and reliable in comparison with the others.

Table 2: The DTMDI optimization results using different metaheuristic algorithms.

SSI Condition	Statistical Parameter	**OSS**	LAPO	SCA	PSO
Fixed base	Best	**22.1769**	24.1952	22.3132	22.4364
	Mean	**22.2002**	29.5791	22.6579	48.8932
	S.D.	**0.0151**	4.0514	0.3221	21.5273
Dense soil	Best	**22.2217**	24.2319	22.3336	22.4575
	Mean	**22.2383**	29.3318	22.6295	49.0114
	S.D.	**0.0101**	3.7491	0.2649	21.6025
Soft Soil	Best	**22.8196**	25.0279	23.0233	23.2074
	Mean	**22.8395**	29.6883	23.3363	51.5716
	S.D.	**0.0090**	4.2320	0.2422	23.0024

The cost function value obtained using LAPO was approximately 9% higher than that of OSS, meanwhile SCA differed by less than 1% and PSO showed deviation of at least 1%, respectively. Consequently, OSS is considered as the most effective algorithm among the treated methods.

The results also indicate that, based on the optimal values derived from the algorithms, and particularly by OSS, the objective function increases as the soil becomes softer. Specifically, transitioning from fixed base to dense soil has resulted in rising up the values by less than 1%, while shifting from fixed base to soft soil has led to nearly 3% increase.

The convergence behavior of each algorithm for different soil conditions is illustrated in Fig.2. Given the superior performance of the OSS algorithm, its optimized parameters were used in subsequent analyses. These optimized DTMDI parameters for each soil type are reported in Table 3.

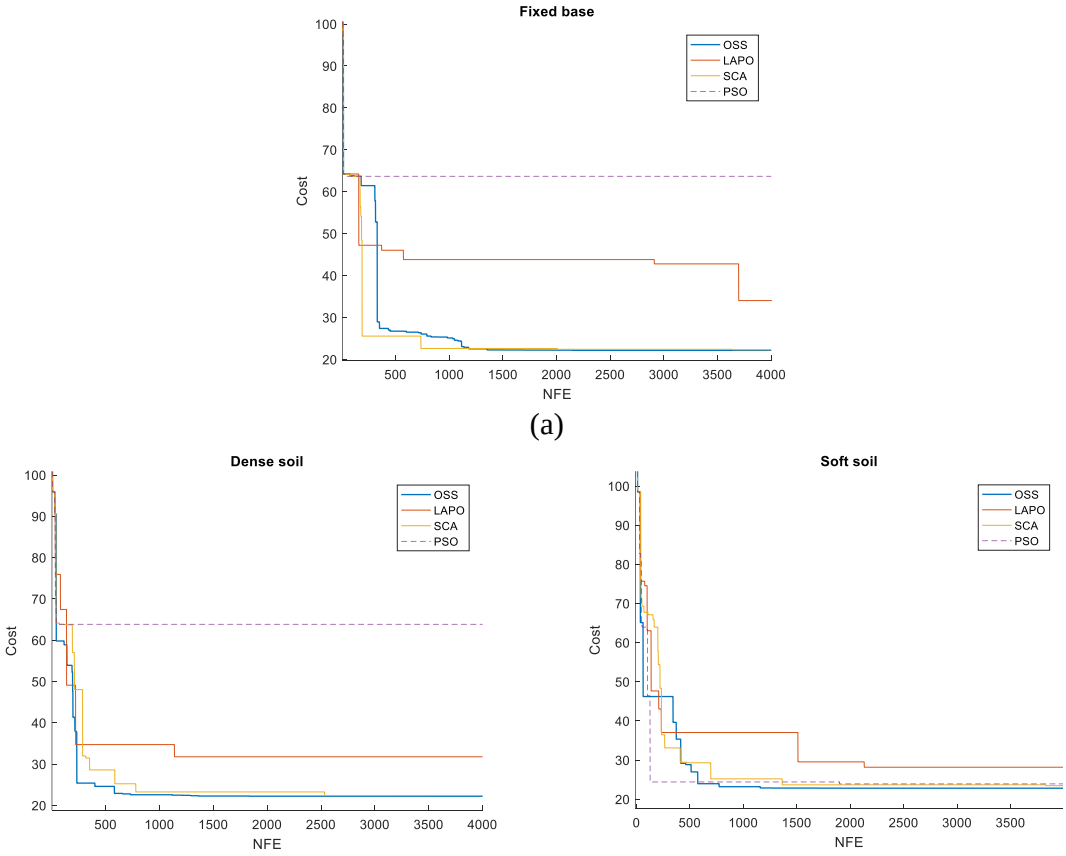

Figure 2: Convergence of the applied methods for: (a) fixed base, (b) dense soil, and (c) soft soil

Fig. 3 displays the frequency-domain roof displacement responses for fixed base, dense, and soft soils. It is evident that the DTMDI system significantly reduced the peak structural response across all SSI conditions, compared with the uncontrolled case. Furthermore, the system showed better performance in reducing the objective function at lower frequencies, while maintaining a response behavior similar to that of the uncontrolled structure, which highlights the inherent stability of the DTMDI system.

Table 3: Optimal DTMDI parameters by OSS for different SSI conditions.

SSI condition	Prescribed Parameters		Optimum parameters			
	$\mu_1 = \mu_2$	β	f_{d1}	ξ_{d1}	f_{d2}	ξ_{d2}
Fixed base	0.0050	0.1000	0.2902	0.0000	0.0100	1.3303
Dense soil	0.0050	0.1000	0.2899	0.0281	0.0100	0.4327
Soft soil	0.0050	0.1000	0.2901	0.0274	0.0105	0.4164

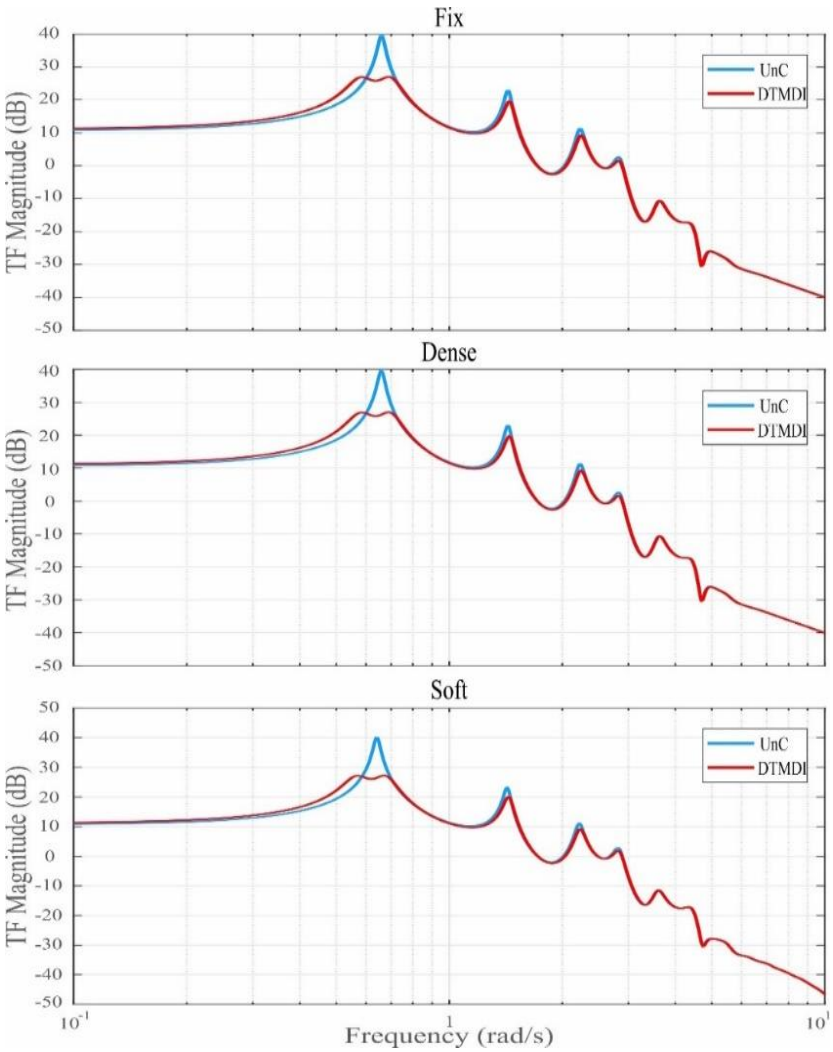

Figure 3: Frequency response of the controlled and uncontrolled systems for 3 SSI conditions

5. NUMERICAL MODELING

To evaluate effectiveness of the DTMDI system, a 15-story shear building [32] is modeled

considering soil–structure interaction. Mass and stiffness quantities of each story are listed in Table 4. The damping matrix is generated using 2% inherent damping via classical Rayleigh method. The dynamic properties of the soil models are summarized in Table 5.

Table 4: Mass and stiffness values of the 15-story building [32].

Story	Mass ($10^6 kg$)	Stiffness ($10^8 N/m$)	Story	Mass ($10^6 kg$)	Stiffness ($10^8 N/m$)	Story	Mass ($10^6 kg$)	Stiffness ($10^8 N/m$)
1	2.11	2.16	6	1.97	0.59	11	1.64	0.25
2	2.15	1.36	7	1.95	0.51	12	1.35	0.19
3	2.13	1.02	8	1.94	0.43	13	1.80	0.10
4	2.13	0.82	9	1.87	0.37	14	0.74	0.07
5	2.04	0.69	10	1.74	0.31	15	0.51	0.04

Time-domain analysis was conducted using real earthquake ground motions, categorized into three sets of seven records: far-field, near-field with forward directivity, and near-field with fling-step effects. Table 6 gives specification of such ground motion records.

Table 5: Soil stiffness and damping parameters [33].

Soil type	Swaying damping $C_h(N.s/m)$	Rocking damping $C_\theta(N.s/m)$	Swaying stiffness $K_h(N/m)$	Rocking stiffness $K_\theta(N/m)$
Dense soil	$4{,}99 \times 10^8$	$1{,}65 \times 10^{10}$	$3{,}31 \times 10^{10}$	$3{,}63 \times 10^{12}$
Soft soil	$7{,}48 \times 10^7$	$2{,}47 \times 10^9$	$1{,}10 \times 10^9$	$1{,}43 \times 10^{11}$

Two performance indices were defined to evaluate the system response in the time domain: J_1 as the normalized peak roof displacement and J_2 being the normalized peak roof acceleration; each one representing the ratio of the controlled to uncontrolled response. Such performance indices are defined as:

$$J_1 = \frac{\max|x_c(t)|}{\max|x_u(t)|} \tag{25}$$

$$J_2 = \frac{\max|\ddot{x}_c(t)|}{\max|\ddot{x}_u(t)|} \tag{26}$$

The subscripts ***c*** and ***u*** in Equations (25) and (26), correspond to the controlled and uncontrolled cases, respectively.

Table 6: Properties of the applied earthquake records [34].

#	Earthquake	Date	Mw	Station	Component angle	PGA (g)
Far-field records						
1	Kern County	1952	7.5	Taft	111	0.18
2	Imperial Valley	1979	6.5	calexico	225	0.27
3	Loma Prieta	1989	7.0	Presido	00	0.10
4	Northridge	1994	6.7	Century CCC	90	0.26
5	Northridge	1994	6.7	Moorpark	180	0.29
6	Northridge	1994	6.7	Montebello	206	0.18
7	San Fernando	1971	6.6	Castaic	291	0.27
Near-field records (Forward-Rupture Directivity)						
8	Cape Mendocino	1992	6.5	Petrolia	90	0.66
9	Northridge	1994	6.5	Olive View	360	0.84
10	Erzincan	1992	6.7	Erzincan	EW	0.50
11	Parkfield	2004	7.3	Fault Zone 1	90	0.50
12	Morgan Hill	1984	6.7	Anderson Dam	340	0.29
13	Superstition Hills	1987	6.7	Parachute Test site	315	0.384
14	Imperial-Valley	1979	7.5	Brawley Airport	225	0.16
Near-field records (Fling-Step)						
15	Kocaeli	1999	6.8	Yarimca	060	0.32
16	Chi-Chi	1999	6.5	TCU052	NS	0.44
17	Chi-Chi	1999	6.8	TCU068	EW	0.50
18	Chi-Chi	1999	6.9	TCU074	EW	0.59
19	Chi-Chi	1999	7.0	TCU084	EW	0.98
20	Chi-Chi	1999	6.5	TCU102	EW	0.29
21	Chi-Chi	1999	7.5	TCU128	EW	0.14

Table 7 presents the computed performance criteria for each ground motion and soil condition. The results confirm that the DTMDI system has effectively reduced both displacement and acceleration at the roof level across all records and soil types. The mean values of J_1 under far-field, forward-directivity near-field, and fling-step near-field records were 0.850, 0.906, and 0.903 for the fixed base; 0.855, 0.909, and 0.904 for the dense soil; and 0.878, 0.914, and 0.901 for the soft soil, respectively.

The results indicate that the system yielded better performance under far-field records compared to both types of near-field excitations. Additionally, the average performance under fling-step records was slightly better than that under forward-directivity records. It was observed that for far-field and forward-directivity records, the normalized displacement

increased with soil flexibility, while under fling-step records, the soft soil condition resulted in better performance than the fixed base and dense soil cases.

Table 7: Performance indices under different SSI conditions and ground motion records.

#	Fixed base		Dense soil		Soft soil	
	J_1	J_2	J_1	J_2	J_1	J_2
Far-fault records						
1	0.6773	0.9593	0.6315	0.9857	0.6800	0.9878
2	0.8928	0.9023	0.8949	1.0000	0.8659	0.9797
3	0.8370	0.9712	0.8401	0.9717	0.9255	1.0074
4	0.9514	0.9629	0.9538	0.9849	0.9582	0.9872
5	0.8631	0.9745	0.8687	0.9847	0.9139	0.9876
6	0.8600	0.9683	0.8617	0.9960	0.8619	0.9970
7	0.9314	0.9799	0.9346	1.0000	0.9411	1.00
Near-Fault records (Forward-Rupture Directivity)						
8	0.9298	0.9591	0.9325	0.9701	0.9352	0.9728
9	0.9423	0.9609	0.9443	0.9776	0.9463	0.9855
10	0.9247	0.9565	0.9275	0.9660	0.9309	0.9512
11	0.8802	0.9411	0.8841	0.9995	0.8977	0.9995
12	0.9451	0.9584	0.9479	0.9998	0.9511	0.9982
13	0.9064	0.9447	0.9096	0.9533	0.9162	0.9544
14	0.8163	0.9499	0.8190	0.9598	0.8245	0.9609
Near-Fault records (Fling-Step)						
15	0.9188	0.9422	0.9193	0.9461	0.9201	0.9493
16	0.9504	0.9573	0.9503	0.9896	0.9482	0.9882
17	0.8990	0.9072	0.8989	0.9072	0.8912	0.9117
18	0.9561	0.9852	0.9586	0.9879	0.9550	0.9898
19	0.9306	0.9740	0.9323	0.9549	0.9322	0.9527
20	0.8606	0.9504	0.8616	0.9391	0.8575	0.9589
21	0.8040	0.8855	0.8052	0.8864	0.8025	0.9018

Regarding the acceleration response, the mean values of J_2 under far-field, forward-directivity, and fling-step records were 0.960, 0.953, and 0.943 for fixed base; 0.989, 0.975, and 0.944 for dense soil; and 0.993, 0.975, and 0.950 for soft soil, respectively. These results delcare that peak roof accelerations were generally higher for far-field records. The fling-step records yielded the lowest acceleration values among the three sets, and with the exception of the forward-directivity group—where soft and dense soils exhibited similar results—the acceleration increased with soil softness.

In general, the optimum DTMDI-controlled structure demonstrated superior performance in reducing both peak displacement and acceleration. Nearly in none of the cases did the controlled responses exceed those of the uncontrolled structure, except for a single instance under the record number 3 in soft soil, where the peak acceleration was approximately 1% higher at few time increments. Fig. 4 illustrates the time histories of roof displacement and acceleration responses under the record number 3 for all the treated SSI conditions.

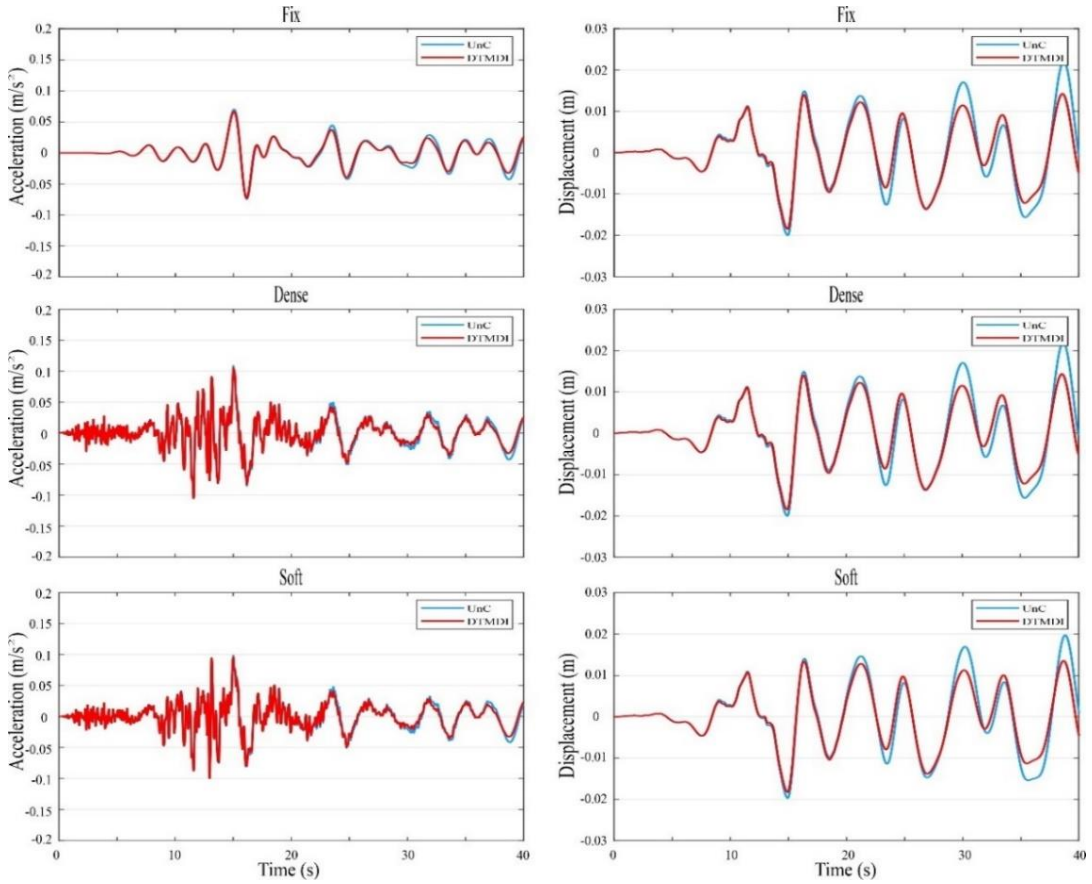

Figure 4: The roof displacement and acceleration time histories under the record #3

6. CONCLUSION

The present study offered optimal configuration of a Double Tuned Mass Damper Inerter (DTMDI) system applied to a 15-story building as a case study with 2% inherent damping, taking into account soil–structure interaction effects. Three parameter-less and one most popular metaheuristic algorithms were compared in optimization of DTMDI parameters, with an objective function independent from random variation of the seismic excitations.

Considering both a position and its opposite, empowered OSS to more efficiently explore the search space. According to the results, OSS showed superior performance in optimal design of DTMDI over SCA, LAPO and PSO. It stands on the first rank not only in the best results but also in the mean and standard deviation showing robust performance and stable convergence with overpassing local optima. The proposed OSS is also of practical interest; being a parameter-less algorithm that avoids extra tuning burden for extra parameters rather than just the population size and the prescribed number of function evaluations.

The results from both frequency-domain and time-domain analyses demonstrated that the DTMDI system was effective in reducing the seismic responses across all three SSI conditions; i.e. the fixed base, the dense and the soft soil. Time-domain analyses were

conducted under a variety of far-field, forward-directivity near-field, and fling-step near-field earthquake records. According to the normalized indices the greatest average reduction in the displacement occurred under far-field records, while the highest average reduction in acceleration was achieved under fling-step records.

It is forth notifying that in none of the cases, the controlled response exceeded that of the uncontrolled structure. The matter underscores the robustness and reliability of the proposed DTMDI system under diverse geotechnical and seismic conditions.

In conclusion, the present work confirmed the effectiveness of the DTMDI system in mitigating seismic responses in buildings with soil–structure interaction, and highlighted the essential role of intelligent optimization algorithms in the design of advanced passive control devices.

REFERENCES

1. Casciati F, Van Der Eijk C. Variability in mechanical properties and microstructure characterization of CuAlBe shape memory alloys for vibration mitigation. *Smart Struct Sys.* 2008;**4**:103–21.
2. Bekdaş G, Kayabekir AE, Nigdeli SM, Toklu YC. Tranfer function amplitude minimization for structures with tuned mass dampers considering soil-structure interaction. *Soil Dyn Earthq Eng.* 2019;**116**:552–62.
3. Kaveh A, Javadi SM, Mahdipour Moghanni R. Optimal structural control of tall buildings using tuned mass dampers via chaotic optimization algorithm. *Structures*. 2020;**28**:2704–13.
4. Kaveh A. *Advances in Metaheuristic Algorithms for Optimal Design of Structures*. 3rd ed. Cham: Springer International Publishing; 2021.
5. Shahrouzi M, Farahabadi H. A fast fuzzy-tuned multi-objective optimization for sizing problems. *Int J Optim Civil Eng.* 2018;**8**:53–75.
6. Shahrouzi M, Sazjini M. Refined harmony search for optimal scaling and selection of accelerograms. *Sci Iran*. 2012;**19**:218–24.
7. Dokeroglu T, Sevinc E, Kucukyilmaz T, Cosar A. A survey on new generation metaheuristic algorithms. *Comput Indust Eng*. 2019;**137**:106040.
8. Shahrouzi M, Rafiee-Alavijeh F, Aghabaglou M. Configuration design of structures under dynamic constraints by a hybrid bat algorithm and teaching–learning based optimization. *Int J Dyn Control*. 2019;**7**:419–29.
9. Kamgar R, Khatibinia M, Khatibinia M. Optimization criteria for design of tuned mass dampers including soil–structure interaction effect. *Int J Optim Civil Eng.* 2019;**9**:213–32.
10. Kaveh A, Mohammadi S, Khadem Hosseini O, Keyhani A, Kalatjari VR. Optimum parameters of tuned mass dampers for seismic applications using charged system search. *Iran J Sci Tech* - C1. 2015;**39**:21–40.
11. Bekdaş G, Nigdeli SM, Yang XS. Metaheuristic based optimization for tuned mass dampers using frequency domain responses. In: Del Ser J, editor. *Advances Intell Sys Comput*, Singapore: Springer Singapore; 2017; **514:** 271–9.
12. Khatibinia M, Gholami H, Labbafi SF. Multi – Objective Optimization of Tuned Mass Dampers Considering Soil–Structure Interaction. *Int J Optim Civil Eng.* 2016;**6**:595–610.

13. Marian L, Giaralis A. Optimal design of a novel tuned mass-damper-inerter (TMDI) passive vibration control configuration for stochastically support-excited structural systems. *Prob Eng Mech*. 2014;**38**:156–64.
14. Smith MC. Synthesis of mechanical networks: The inerter. *IEEE Tran Auto Control*. 2002;**47**:1648–62.
15. Dai J, Xu Z-D, Gai P-P. Tuned mass-damper-inerter control of wind-induced vibration of flexible structures based on inerter location. *Eng Struct*. 2019;**199**:109585.
16. Tiwari ND, Gogoi A, Hazra B, Wang Q. A shape memory alloy-tuned mass damper inerter system for passive control of linked-SDOF structural systems under seismic excitation. *J Sound Vib*. 2021;**494**:115893.
17. Rajana K, Giaralis A. A hybrid nonlinear rooftop isolated tuned mass damper-inerter system for seismic protection of building structures. *Int Conf on Natural Hazards Infrastruct.* 2022.
18. Djerouni S, Abdeddaim M, Elias S, Rupakhety R. Optimum Double Mass Tuned Damper Inerter for Control of Structure Subjected to ground motions. *J Build Eng.* 2021;**44**:103259.
19. Jalali HH, Farzam MF. Inerter-Connected Double Tuned Mass Damper for Passive Control of Buildings under Seismic Excitation. *Period Polytech Civil Eng*. 2022;**66**:421–32.
20. Elias S, Djerouni S. Optimum tuned mass damper inerter under near-fault pulse-like ground motions of buildings including soil-structure interaction. *J Build Eng.* 2024;**85**:108674.
21. Shahrouzi M. Optimal Spectral Matching of Strong Ground Motion by Opposition-Switching Search. EngOpt: *6th Int Conf Eng Optim*, Lisbon, Springer International Publishing; 2019; 713–24.
22. Shahrouzi M, Salehi A. Design of Large-Scale Structures by an enhanced Metaheuristic utilizing Opposition-based Learning. CSIEC: 2*020 4th Conf Swarm Intell and Evolut Comput*, Mashhad: *IEEE*; 2020; 27–31.
23. Shahrouzi M, Barzigar A, Rezazadeh D. Static and Dynamic Opposition-based Learning for Colliding Bodies Optimization. *Int J Optim Civil Eng.* 2019;**9**:499–523.
24. Nematollahi AF, Rahiminejad A, Vahidi B. A novel physical based meta-heuristic optimization method known as Lightning Attachment Procedure Optimization. *Appl Soft Comput*. 2017;**59**:596–621.
25. Mirjalili S. SCA: A Sine Cosine Algorithm for solving optimization problems. *Knowledge-Based Sys*. 2016;**96**:120–33.
26. Kennedy J, Eberhart R. Particle swarm optimization. ICNN'95: *Int Conf Neural Net*, *IEEE*; 1942–8.
27. Shahrouzi M, Taghavi AM. A Modified Sine-Cosine Algorithm with Dynamic Perturbation for Effective Optimization Of Engineering Problems. *Int J Optim Civil Eng.* 2024;**14**:385–422.
28. Shahrouzi M. Switching teams algorithm for sizing optimization of truss structures. *Int J Optim Civil Eng*. 2020;**10**:365–89.
29. Shahrouzi M, Kaveh A. An efficient derivative-free optimization algorithm inspired by avian life-saving manoeuvres. *J Comput Sci*. 2022;**57**:101483.
30. Tizhoosh. Reinforcement Learning Based on Actions and Opposite Actions. IN International Conference on Artificial Intelligence and Machine Learning 2005:19–21.
31. Rojas-Morales N, Riff Rojas MC, Montero Ureta E. A survey and classification of

Opposition-Based Metaheuristics. *Comput Indust Eng*. 2017;**110**:424–35.
32. Lavasani SHH, Doroudi R. Meta heuristic active and semi-active control systems of high-rise building. *Int J Struct Eng*. 2020;**10**:232–53.
33. Hosseini Lavassani SH, Shangapour S. Interval Type-2 Fuzzy Hybrid Control of a High-Rise Building Including Soil–Structure Interaction Under Near-Field and Far-Field Ground Motions. *Struct Eng Int*. 2022;**32**:316–27.
34. Hojat Jalali H, Fahimi Farzam M, Mousavi Gavgani SA, Bekdaş G. Semi-active control of buildings using different control algorithms considering SSI. *J Build Eng*. 2023;**67**:105956.

APPENDIX 1: A MATLAB code for the OSS algorithm

```
% ING
%
% Opposition-Switching Search
% by Mohsen Shahrouzi
%
% Ref: http://dx.doi.org/10.1007/978-3-319-97773-7_63
%
function [Gbest,GbestCost]=OSS(PrbInfo,InitPop,NFE_Max)
sz=size(PrbInfo.xLB);
xMat=InitPop.xMat; % Externally initiated population
Costs=InitPop.Costs;
PopSize=size(xMat,1);
GbestCost=inf;
for i=1:PopSize
    if Costs(i)<=GbestCost
        Gbest=xMat(i,:);
        GbestCost=Costs(i);
    end
end
NFE=PopSize;
% + + + main loop + + +
while NFE<NFE_Max
    for i=1:PopSize
        for j=1:numel(xLB);
            jj=randi(PopSize);
            Y(j)=xMat(jj,j);
        end
        r1=rand;        Z=(r1<=0.5)*Y+(r1>0.5)*(PrbInfo.xLB+PrbInfo.xUB-Y);
        V1=rand(sz).*(Gbest-Z);
        x=xMat(xInd,:);
        xD=PrbInfo.xLB+PrbInfo.xUB-x;
        r2=rand;        V2=rand(sz).*((r2<=0.5)*(Gbest-x)-(r2>0.5)*(Gbest-xD));
        Xc=max(PrbInfo.xLB,min(PrbInfo.xUB,x+V1+V2));    % The candidate X
        CostXc=Fcost(Xc); NFE=NFE+1;
        if CostXc<Costs(i),xMat(i,:)=Xc; Costs(i)=CostXc; end
        if CostXc<GbestCost,    Gbest=Xc;GbestCost=CostXc; end
        if NFE==NFE_Max, break,end
    end
end
```